

Probability based comparison of retrofit methods for existing nonductile concrete frames

Andrea Miano¹, Halil Sezen², Fatemeh Jalayer³, and Andrea Prota⁴

¹PhD Candidate, Department of Structures for Engineering and Architecture, University of Naples “Federico II”, andrea.miano@unina.it

²Professor, Department of Civil, Environmental & Geodetic Engineering, Ohio State University

³Associate Prof., Department of Structures for Engineering and Architecture, Univ of Naples “Federico II”

⁴Full Prof., Department of Structures for Engineering and Architecture, Univ of Naples “Federico II”

ABSTRACT: In different high seismic regions around the world, many nonductile existing reinforced concrete frame buildings, built without adequate seismic detailing requirements, have been damaged or collapsed after past earthquakes. These concrete frame buildings are much more susceptible to collapse than modern code-conforming frames. Therefore, for this type of structures, it is necessary to accurately model materials and members to capture the flexure, shear and flexure-shear failure modes in members and the potential collapse of the structure. In this paper, alternative retrofit methods are evaluated for these older frame buildings using a nonlinear structural performance assessment methodology. As a case study, the transverse frame of an existing building is modeled, including the effect of flexural-shear-axial load interaction and the bar slip deformation component to be able to capture also column shear and axial failures. A framework for probability-based demand and capacity factor design (DCFD) seismic safety evaluation is implemented in order to evaluate the structural performance at each chosen performance level. This study shows that it is a critical issue to choose the most effective retrofit strategy based on the assessed performance of the bare frame. Moreover, the estimates of expected life cycle cost are compared for the retrofit methods considered in this research.

KEYWORDS: Performance-based assessment, Seismic retrofit of RC structures, Flexural-shear-axial load interaction, Life cycle cost.

1 INTRODUCTION

Recent devastating earthquakes around the world showed the vulnerability and deficiencies of existing reinforced concrete (RC) frame structures. These concrete frame buildings are much more susceptible to collapse than modern code-conforming frames. Since such buildings comprise large percentage of existing building stock, effective retrofit methods are needed to improve their structural performance and prevent collapse. Depending on the desired performance, conventional retrofit methods, such as concrete or steel jacketing of the columns, addition of shear walls or strengthening beams and columns using new materials, e.g., fiber reinforced polymers (FRP), can be used to meet the new seismic code requirements. In this paper, alternative retrofit methods are evaluated for older nonductile frame buildings using a nonlinear structural performance assessment methodology. Nonlinear dynamic analysis procedures can be used to perform probabilistic seismic assessment, using recorded ground motions. These procedures can be used to estimate parameters required for specific probabilistic assessment criteria, such as Demand and Capacity Factored Design (DCFD, Cornell et al. 2002), and also to make direct probabilistic performance assessment using numerical methods (Shome et al. 1998, Jalayer and Cornell 2009). In particular, Cloud Analysis is chosen here by applying simple

regression in the logarithmic space of nonlinear dynamic structural response versus seismic intensity for a set of ground motion records. The simplicity of its formulation makes it a quick and efficient analysis procedure for fragility assessment and/or performance based safety-checking (Celik and Ellingwood 2010, Jalayer et al. 2007). Based on this probabilistic nonlinear dynamic analysis framework, a risk based retrofit strategy optimization is developed in this study. The structural performance is the main parameter taken in to account for the optimization, although a very brief cost analysis is also presented. A seven-story hotel building in Van Nuys, California, is used as a case study in this research. The RC frame building suffered significant damage during the 1994 Northridge earthquake. A perimeter transverse frame of the building is modeled as built and retrofitted, including the effect of flexural-shear-axial load interaction to be able to capture column shear and axial failures.

2 METHODOLOGY

2.1 The structural performance variable

As described in Jalayer et al. (2007), for each nonlinear time-history analysis, the corresponding critical demand to capacity ratio (DCR_{PL}), equal to the mechanism that brings the structure closest to the onset of the performance level PL , is adopted as the structural response parameter. The DCR_{PL} parameter, that is equal to unity at the onset of performance level, can account for both ductile and brittle failure mechanisms. It is defined as:

$$DCR_{PL} = \max_l^{N_{mech}} \min_j^{N_l} \frac{D_{jl}}{C_{jl}(PL)} \quad (1)$$

where N_{mech} is the number of considered potential failure mechanisms; N_l is the number of components taking part in the l th mechanism; D_{jl} is the demand evaluated for the j th structural component of the l th mechanism; $C_{jl}(PL)$ is the performance level capacity for the j th component of the l th mechanism. The capacity values refer to the Immediate Occupancy PL, Life Safety PL and Collapse Prevention PL Table C2.1 of ASCE 41 (2013) in this work, but the procedure can be used for any other prescribed performance levels or limit states. In DCR_{PL} definition, D is the demand expressed in terms of maximum chord rotation for the component, denoted as $\theta_{D,max}$, and computed from nonlinear dynamic analysis, while for C : a) Immediate Occupancy Performance Level: C is the component chord rotation capacity, denoted as $\theta_{C,yielding}$, and identified as the deformation capacity corresponding to the point in the force-deformation curve of the member in which the longitudinal steel rebar in the member starts to yield in tension; b) Life Safety Performance Level: C is the component chord rotation capacity, denoted as $\theta_{C,ultimate}$, and identified as deformation capacity corresponding to the point in the force-deformation curve of the member, where a 20% reduction in the maximum strength takes place; c) Collapse Prevention Performance Level: C is the component chord rotation capacity, denoted as $\theta_{C,axial}$, and identified as the deformation capacity corresponding to the point in the force-deformation curve of the member associated with the complete loss of vertical-load carrying capacity (to account for the loss of load bearing capacity).

2.2 Cloud Analysis considering collapse and/or global dynamic instability

In order to estimate the structural fragility, *Cloud* analysis is adopted herein as nonlinear dynamic analysis procedures (Jalayer et al. 2015 and 2017). Cloud analysis is a procedure in which a structure is subjected to a set of ground motion records of different first-mode $Sa(T)$ values. Once the ground motion records are selected, they are applied to the structure and the resulting DCR is calculated. This provides a set of values that form the basis for the cloud-method calculations. The cloud data can be separated to two parts: (a) *NoC* data which correspond to that portion of records for which the structure does not experience “*Collapse*”, (b) *C* data for which the structure leads to “*Collapse*” (the criteria for defining Collapse cases are presented in Miano et al. 2017 and 2017b). In order to estimate the statistical properties of the cloud response, with

respect to NoC data, conventional linear regression is applied to the response on the natural logarithmic scale, which is the standard basis for the underlying log-normal distribution model. This is equivalent to fitting a power-law curve to the cloud response in the arithmetic scale. This results in a curve that predicts the median drift demand for a given level of structural acceleration:

$$\begin{aligned}\eta_{DCR|S_a, NoC}(Sa) &= a \cdot Sa^b \\ \ln(\eta_{DCR|S_a, NoC}(Sa)) &= \ln(a) + b \cdot \ln(Sa)\end{aligned}\quad (2)$$

where $\ln(a)$ and b are regression constants. The logarithmic standard deviation $\beta_{DCR|S_a, NoC}$ is the root mean sum of the square of the residuals with respect to the regression prediction:

$$\beta_{DCR|S_a, NoC} = \sqrt{\frac{\sum (\ln(DCR_i) - \ln(a \cdot S_{a,i}^b))^2}{N_{NoC} - 2}}\quad (3)$$

where DCR_i and $S_{a,i}$ are the demand over capacity ratio values and the corresponding spectral acceleration for record number i within the cloud response set and N_{NoC} is the number of NoC records. The standard deviation of regression, as introduced in the preceding equation, is presumed to be constant with respect to spectral acceleration over the range of spectral accelerations in the cloud. The fragility, expressed generally as the conditional distribution of DCR given S_a , can be expanded with respect to NoC and C data as follows using Total Probability Theorem (see Jalayer and Cornell 2009, Jalayer et al. 2017):

$$P(DCR_{LS} > 1 | S_a) = P(DCR_{PL} > 1 | S_a, NoC) \cdot (1 - P(C | S_a)) + P(DCR_{PL} > 1 | S_a, C) \cdot P(C | S_a)\quad (4)$$

The NoC term $P(DCR > 1 | S_a, NoC)$ is the conditional distribution of DCR given S_a and NoC , and can be described by a lognormal distribution (a widely used assumption that has been verified for cases where the residuals represent unimodal behaviour (Jalayer and Ebrahimiyan 2016):

$$P(DCR_{PL} > 1 | S_a, NoC) = \Phi\left(\frac{\ln \eta_{DCR_{PL}|S_a, NoC}}{\beta_{DCR_{PL}|S_a, NoC}}\right)\quad (5)$$

where Φ is the standardized Gaussian cumulative distribution function (CDF) and $\eta_{DCR|S_a, NoC}$ and $\beta_{DCR|S_a, NoC}$ are presented in Eqs. (2) and (3). The term $P(C | S_a) = 1 - P(NoC | S_a)$ is probability of global dynamic instability (Collapse), which can be expressed by a logistic regression model (a.k.a., logit) on the S_a values of the entire cloud data:

$$P(C | S_a) = \frac{1}{1 + e^{-(\beta_0 + \beta_1 \cdot S_a)}}\quad (6)$$

where β_0 and β_1 are the parameters of the logistic regression. The logistic regression model belongs to generalized regression models and is useful for cases in which the regression dependent variable is binary (i.e., can have only two values 1 and 0, *yes* or *no*, as in the case of C and NoC).

2.3 Performance-based safety-checking framework

As described in Jalayer and Cornell (2003), a framework for probability-based demand and capacity factor design ($DCFD$) seismic safety evaluation is implemented in order to verify the structural safety at each performance level. The $DCFD$ format is based on a closed-form analytical expression for the mean annual frequency of exceeding a structural performance level. The threshold for each performance level is identified by a critical DCR_{PL} calculated for the prescribed performance level and set equal to unity. According to $DCFD$, the structure is safe for a performance level PL if the seismic demand corresponding to an acceptable risk level is less than the seismic capacity for that PL . Herein, an intensity-based version of this format is adopted where the safety criteria is expressed in term of the seismic intensity measure (see Jalayer et al. 2016):

$$S_a(P_o) \leq S_a^{PL}\quad (7)$$

where $S_a(P_o)$ or the IM-based *factored demand* (denoted generically later as D_{PL} , where $PL=IO, LS, CP$) is the spectral acceleration value corresponding to the acceptable probability level P_o ,

based on the site-specific mean hazard curve (<https://www.usgs.gov>) for the fundamental period of the frame. The hazard curve is approximated by a power-law type of expression in the region of spectral acceleration values of interest:

$$S_a(P_o) = \lambda_{S_a}^{-1}(P_o) ; \lambda_{S_a}(S_a) \approx k_o \cdot S_a^{-k} \quad (8)$$

where k_o and k are the fit parameters with k that is the slope of this approximate curve. S_a^{PL} (denoted generically later as C_{PL}) is the IM-based *factored capacity* and is calculated as:

$$S_a^{PL} = \eta(S_a^{DCR_{PL}=1}) \cdot \exp\left(-\frac{k}{2} \beta(S_a^{DCR_{PL}=1})^2\right) \quad (9)$$

where $S_a^{DCR_{PL}=1}$ is the spectral acceleration at the onset of performance level PL ($DCR_{PL}=1$); $\eta(S_a^{DCR_{PL}=1})$ and $\beta(S_a^{DCR_{PL}=1})$ are the median and logarithmic standard deviation of the fragility curve for performance level PL . The fragility, defined as $P(DCR_{PL} > 1 | S_a)$ is a lognormal cumulative distribution function with median and logarithmic standard deviation equal to:

$$\eta(S_a^{DCR_{PL}=1}) = S_a^{50th} ; \beta(S_a^{DCR_{PL}=1}) = \frac{1}{2} \ln \frac{S_a^{84th}}{S_a^{16th}} \quad (10)$$

where S_a^{16th} , S_a^{50th} , S_a^{84th} are the S_a values corresponding to probability of 0.16, 0.50 and 0.84.

3 NUMERICAL APPLICATION

3.1 Building description and flexural model

One of the perimeter transverse frames of the seven-story hotel building in Van Nuys, California, is modeled in this study (Fig. 1a). All columns and beams details are provided in (Krawinkler 2005). The hotel building experienced shear failures in the columns during the 1994 Northridge earthquake. It is necessary to model materials and column members to capture the shear and the flexure-shear failure modes in columns and the potential collapse of the transverse frame (see Miano et al. 2017 b for more details). About flexural model, unidirectional axial behaviour of concrete and steel are modeled to simulate the nonlinear response of beams and columns. Flexural response of beams and columns response is simulated using uniaxial fibers within the gross cross section were assigned either concrete or steel. A typical column cross section included 30 layers of axial fibers, parallel to the depth of the section. In force-based column elements, distributed plasticity model is used in OpenSees in order to allows for yielding and plastic deformations at any integration point along the element length under increasing loads. Newton-Cotes integration (Scott and Fenves 2006), that distributes integration points uniformly along the length of the element, including one point at each end of the element (Fig. 1b), is selected. Beams member force-deformation response is computed assuming that inelastic action occurs at the member ends and that the middle of the member remains elastic. Modified Gauss Radau integration (Scott and Fenves 2006), that presents two integration points at the element ends and at 8/3 of the hinge length, $L_o=h$, from the end of the element (Fig. 1c), is selected.

3.2 Shear and bar slip models

About shear modeling, the shear model by (Setzler and Sezen 2008) can capture the shear response with a lateral force-shear displacement envelope, that includes three distinct points corresponding to: 1) Maximum shear strength and corresponding shear displacement; 2) Onset of shear strength degradation and corresponding displacement; 3) Shear displacement at axial load failure. The shear strength is calculated according to the model by (Sezen 2008). The shear displacement at peak strength is calculated as in Sezen (2008). As described in Setzler and Sezen (2008), the shear displacement at the onset of shear failure is adopted from Gerin and Adebear (2004). Shear displacement at axial failure is obtained through the equation proposed by Elwood and Moehle 2005. About bar slip model, slip of column reinforcing bars at column ends causes rigid body rotation of the column. This rotation is not accounted for in flexural analysis, where

the column ends are assumed to be fixed. The bar slip model used in this study was developed by Sezen and Moehle (2004). This model assumes a stepped function for bond stress between the concrete and reinforcing steel over the embedment length of the bar. The rotation due to slip, θ_s , is calculated as $slip/(d-c)$, where slip is the extension of the outermost tension bar from the column end and d and c are the distances from the extreme compression fiber to the centroid of the tension steel and the neutral axis. The column lateral displacement due to bar slip is equal to the product of the slip rotation and the column length.

3.3 Total lateral response

The total lateral response of a RC column is modeled using a set of springs in series in OpenSees (the flexural spring is the fiber section element). The flexure, shear and bar slip deformation models are modeled by springs in series. Each spring is subjected to the same lateral force. The total displacement response is the sum of the responses of each spring. The column springs model, shown in Fig. 1b, has two zero-length bar slip springs, one zero-length shear spring and a flexural member with five integration points.

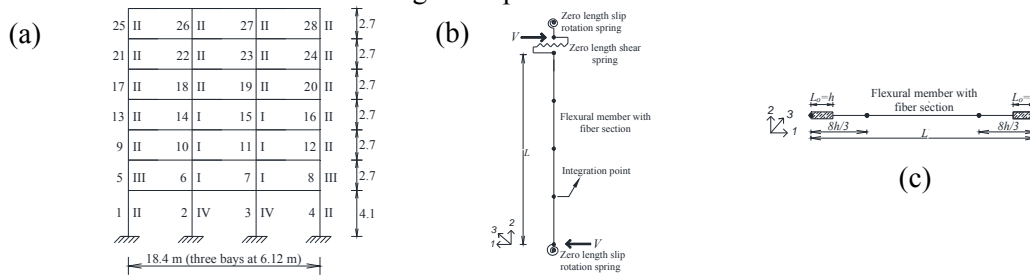


Figure 1. a) Geometric configuration of the transverse, b) columns, and c) beams models.

The three deformation components are added together to predict the total response up to the peak strength of the column. Rules are established for the post-peak behavior of the springs based on a comparison of the shear strength V_n , the yield strength V_y , and the flexural strength V_p . By comparing V_n , V_y , and V_p , the columns are classified into different categories (Setzler and Sezen 2008). Figure 2a shows the three different deformation components and the total lateral displacement for a columns of the frame, belonging to Category I (shear critical members).

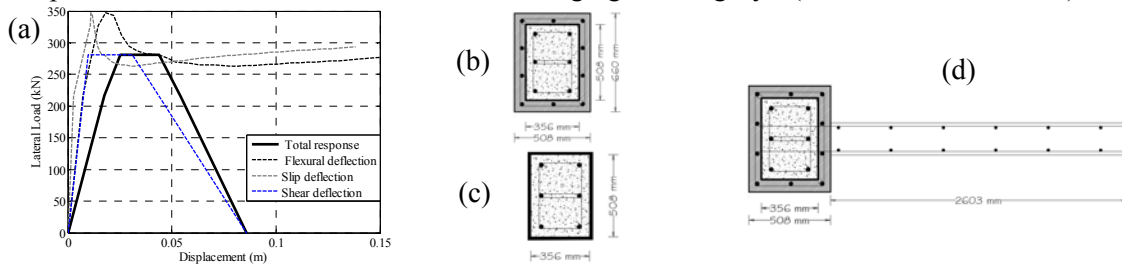


Figure 2 a) Deformation components and total response for a columns of the frame belonging to Category I; b) RC jacketing of columns, c) FRP wrapping of columns, and d) Shear wall addition.

3.4 Retrofit modeling

Three different retrofit schemes have been considered (Miano et al. 2017). The first scheme is the reinforced concrete jacketing of all columns in the frame. The goal is to prevent shear damage in columns and to achieve flexural yielding and sufficient ductility (Fig.2b). The second retrofit method is the addition of a new shear wall into the frame to increase the strength and stiffness and to reduce demand on the unstrengthened columns, limiting the lateral displacement. The wall is centered on the frame and is doweled into the existing columns and beams (Fig.2c). In the third retrofit application, the columns of the frame are wrapped with carbon fiber reinforced polymer composite (CFRP) (Fig.2d) in order to increase shear strength and to prevent shear failure in columns. The CFRP also improves the deformation capacity, by providing confinement.

3.5 Cloud Analysis and performance-based safety-checking results

A set of 70 strong ground-motion records are selected from the NGA-West2 database in order to implement Cloud Analysis. This suite of records is presented in details in Jalayer et al. 2017. Figure 3 shows Cloud Analysis for the life safety performance level for each model and illustrate the 16th, 50th and 84th percentiles of the performance variable as a function of spectral acceleration. The same procedure has been implemented also for the other two performance levels.

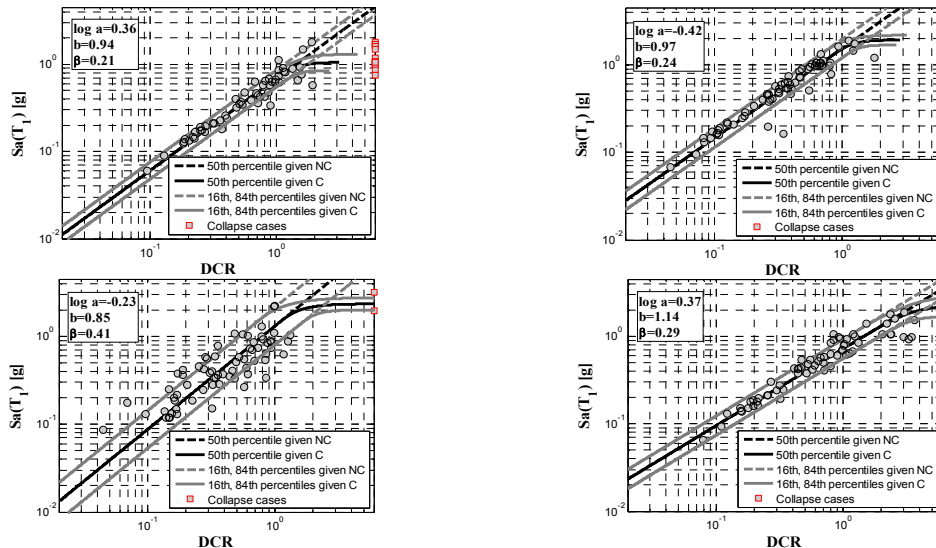


Figure 3 Cloud regression for LS_{PL}: a) bare frame, b) RC jacketing, c) shear wall and d) FRP wrapping.

The results of demand and capacity factor design (DCFD) seismic safety evaluation, are here presented in order to verify the structural safety at each performance level. Table 1 shows the comparison between D_{PL} and C_{PL} , respectively, for each modeling option in each performance level. Figure 4 shows the fragility curves and the calculation of $D_{PL} S_a(P_o)$ and $C_{PL} = S_a^{PL}$. Figure 7a shows the mean hazard curves (<https://www.usgs.gov>), used to calculate D_{PL} .

Table 1 Comparison between DPL and CPL for each modelling option in each performance level.

Model	$S_a(T_1)$ (g)	D_{IO} (g)	C_{IO} (g)	D_{LS} (g)	C_{LS} (g)	D_{CP} (g)	C_{CP} (g)
Bare frame	1.11	0.27	0.30	0.46	0.63	0.80	0.81
RC jacketing	1.01	0.28	0.47	0.48	1.43	0.84	1.84
Shear wall	0.40	0.47	0.53	0.79	1.02	1.33	1.98
FRP wrapping	1.04	0.27	0.33	0.47	0.65	0.82	1.83

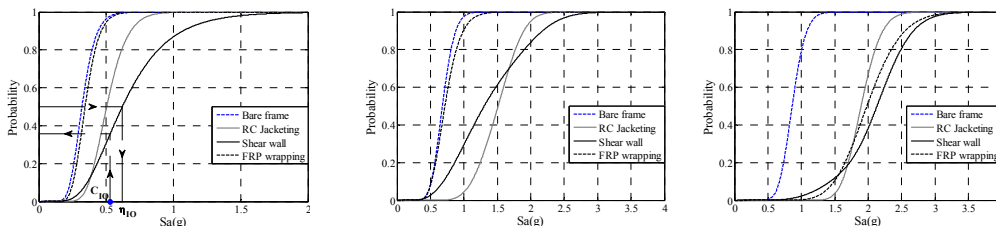


Figure 4 Fragility curves for the three performance levels.

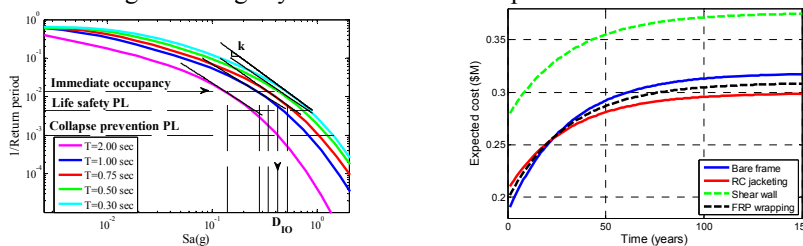


Figure 5 a) Mean hazard curves; b) expected life-cycle cost for bare frame and alternative retrofit options.

4. LIFE CYCLE COST ANALYSIS

The expected life cycle cost is an important parameter for measuring the effectiveness of each retrofit option. In this paper, the expected life cycle cost is estimated as (Wen 2001):

$$\mathbb{E}[C] = C_0 + C_R + C_M \quad (11)$$

where C_0 is the initial construction or upgrade installation cost, C_R is the repair cost considering also the downtime loss, and C_M is the annual maintenance costs. The repair cost C_R is equal to:

$$C_R = \sum_{t=0}^T \sum_{pl=1}^{N_{PL}} PLC \cdot e^{-\lambda_d t} [P(PL|[t, t+1]) - P(PL+1|[t, t+1])] \quad (12)$$

where N_{PL} is the number of performance levels; PLC is the expected cost of restoring the structure from the pl th performance level back to its intact state; λ_d is the annual discount rate and $\exp(-\lambda_d t)$ denotes the change in the monetary-based evaluations per time; $P(PL|[t, t+1])$ is the probability of exceeding the pl in time interval $[t, t+1]$. $P(PL|[t, t+1])$ can be calculated as:

$$P(PL|[t, t+1]) = \lambda_{pl} \exp(-\lambda_{pl} t) \quad (13)$$

where λ_{pl} is the mean annual rate of exceeding the performance level pl and can be calculated from the following closed-form expression (Jalayer and Cornell 2003):

$$\lambda_{pl} = \lambda_{S_a} (\eta(S_a^{DCR_{pl}=1})) \cdot \exp\left(\frac{k^2}{2} \cdot \beta(S_a^{DCR_{pl}=1})^2\right) \quad (14)$$

where $\lambda_{S_a}(\eta(S_a^{DCR_{pl}=1}))$ is the hazard value for the median S_a at the onset of pl . PLC is equal to:

$$PLC = DTC \cdot e^{-\lambda_d \tau_{pl}} + RC_{pl} \quad (15)$$

where DTC is the annual cost of downtime; τ_{pl} is the repair time (Comerio 2006) and RC_{pl} is the replacement cost for the pl th performance level. The cost of maintenance C_M can be estimated as:

$$C_M = \int_0^{life} C_m e^{-\lambda_d t} dt = (C_m / \lambda_d) \cdot [1 - e^{-\lambda_d life}] \quad (16)$$

where C_m is the constant annual maintenance cost. Table 2 outlines the values used for C_0 (Liel et al. 2013, Vitiello et al. 2016), RC_{IO} , RC_{LS} , RC_{CP} (Liel et al. 2013, FEMA 2003) DTC and C_m (Ebrahimian et al. 2015). Figure 5b shows the expected life-cycle cost results.

Table 2 Life-cycle cost analysis parameters.

Retrofit Option	C_0 ($\cdot 10^5$, \$)	DTC ($\cdot 10^5$, \$/year)	RC_{IO} (\$/year)	RC_{LS} (\$/year)	RC_{CP} ($\cdot 10^5$, \$/year)	C_m ($\cdot C_0$, \$/year)
Bare frame	1.86	2.73	0.1· RC_{CP}	0.5· RC_{CP}	2.34	0.01
RC Jacketing	2.07	2.73	0.1· RC_{CP}	0.5· RC_{CP}	2.34	0.01
Shear wall	2.77	2.73	0.1· RC_{CP}	0.5· RC_{CP}	2.34	0.01
FRP wrapping	1.98	2.73	0.1· RC_{CP}	0.5· RC_{CP}	2.34	0.01

5. CONCLUSIONS

In this paper, alternative retrofit methods are evaluated for older nonductile frame buildings using a nonlinear structural performance assessment methodology. The structural performance is the main parameter considered for the optimization, although a cost analysis is presented to compare the estimates of expected life cycle cost for the retrofit methods. In the assessment is fundamental to accurately model materials and column members (considering also specific shear and slip models) to capture flexure, shear and flexure-shear failure modes in columns and the potential collapse of the building. The final results show that each retrofit strategy improves the performance of the existing building differently based on how much it increases ductility and strength, avoiding brittle mechanisms. For the case study, RC jacketing of the columns seems to be the most effective retrofit option based on structural and life cycle cost results. However, the novelty of the proposed research is not in the choice of the best retrofit option for existing RC buildings, but it is in the critical process presented to evaluate the effectiveness of different retrofit methods using a performance based approach.

References

- American Society of Civil Engineers 41. (2013), Seismic Evaluation and Retrofit of Existing Buildings.
- Celik OC and Ellingwood BR. (2010), Seismic fragilities for non-ductile reinforced concrete frames–Role of aleatoric and epistemic uncertainties. *Structural Safety* 32(1): 1-12.
- Comerio MC. (2006), Estimating downtime in loss modeling. *Earthquake Spectra* 22.2: 349-365.
- Cornell CA Jalayer F Hamburger RO and Foutch DA. (2002), Probabilistic basis for 2000 SAC federal emergency management agency steel moment frame guidelines. *Journal of Struc Eng*, 128(4), 526-533.
- Elwood KJ and Moehle JP. (2005), Axial capacity model for shear-damaged columns. *ACI Structural Journal* 102, 578-587.
- Fema, Hazus-Mh. (2003), MR3 Technical Manual: Multi-hazard loss estimation methodology earthquake model.
- Gerin M and Adebar P. (2004), Accounting for shear in seismic analysis of concrete structures. Proc., 13th World Conference on Earthquake Engineering, 1-6.
- Galanis PH and Moehle JP. (2015), Development of collapse indicators for risk assessment of older-type reinforced concrete buildings. *Earthquake Spectra*, 31(4), 1991-2006.
- Ebrahimian H Jalayer F and Manfredi G. (2015). Seismic retrofit decision-making of bridges based on life cycle cost criteria. *COMPdyn* 2015.
- Jalayer F and Cornell CA. (2003), A technical framework for probability-based demand and capacity factor design (DCFD) seismic formats. Technical Report PEER 2003/08, Berkeley, USA.
- Jalayer F Franchin P and Pinto P. (2007), A scalar damage measure for seismic reliability analysis of RC frames. *Earthquake Engineering & Structural Dynamics*, 36(13), 2059-2079.
- Jalayer F and Cornell CA. (2009), Alternative non-linear demand estimation methods for probability-based seismic assessments. *Earthquake Engineering & Structural Dynamics* 38(8): 951-972.
- Jalayer F De Risi R Manfredi G. Bayesian Cloud Analysis: efficient structural fragility assessment using linear regression. *Bull Earthq Eng*. 2015; 13(4):1183-1203.
- Jalayer F Carozza S De Risi R Manfredi G and Mbuya E. (2016), Performance-based flood safety-checking for non-engineered masonry structures. *Engineering Structures*, 106, 109-123.
- Jalayer F and Ebrahimian H. (2016), Seismic risk assessment considering cumulative damage due to aftershocks. *Earthquake Engineering & Structural Dynamics*.
- Jalayer F Ebrahimian H Miano A Manfredi G and Sezen H. Analytical fragility assessment using un-scaled ground motion records. *Earthquake Engineering & Structural Dynamics*, 1-25, D.O.I: 10.1002/eqe.2922.
- Krawinkler H. (2005), Van Nuys hotel building testbed report: exercising seismic performance assessment. Pacific Earthquake Engineering Research Center, Univ. of California, Berkeley.
- Liel AB and Deierlein GG. (2013). Cost-benefit evaluation of seismic risk mitigation alternatives for older concrete frame buildings. *Earthquake Spectra* 29(4): 1391-1411.
- McKenna F. (2011), OpenSees: a framework for earthquake engineering simulation." *Computing in Science & Engineering*, 13(4), 58-66.
- Miano A Sezen H Jalayer F and Prota A. Performance based assessment methodology for retrofit of buildings. *Earthquake Spectra* 2017; (Submitted).
- Miano A Sezen H Jalayer F and Prota A. (2017) b, Performance-based comparison of different retrofit methods for reinforced concrete structures. *Compdyn* 2017.
- Scott MH and Fenves GL. (2006), Plastic hinge integration methods for force-based beam–column elements. *Journal of Structural Engineering*, 132(2), 244-252.
- Setzler EJ and Sezen H. (2008), Model for the lateral behavior of reinforced concrete columns including shear deformations. *Earthquake Spectra*, 24(2), 493-511.
- Sezen H and Moehle JP. (2004), Shear strength model for lightly reinforced concrete columns. *Journal of Structural Engineering*, 130(11), 1692-1703.
- Sezen H. (2008), Shear deformation model for reinforced concrete columns. *Structural Engineering and Mechanics*, 28(1), 39-52.
- Shome N Cornell CA Bazzurro P and Carballo JE. (1998), Earthquakes, records, and nonlinear responses. *Earthquake Spectra*, 14(3), 469-500.
- Vitiello U Asprone, D Di Ludovico M and Prota A. (2017), Life cycle cost optimization of the seismic retrofit of existing RC structures. *Bulletin of Earthquake Engineering*. 15.5, 2245-2271.
- Wen YK. (2001), Reliability and performance-based design. *Structure Safety*, 23(4), 407-428.